Structural Biology Hot Paper

International Edition: DOI: 10.1002/anie.201501742
German Edition: DOI: 10.1002/ange.201501742

The Mechanism of Ligand-Induced Activation or Inhibition of μ- and κ-Opioid Receptors **

Shuguang Yuan, Krzysztof Palczewski, Qian Peng, Michal Kolinski, Horst Vogel,* and Slawomir Filipek**

Abstract: *G-protein-coupled receptors (GPCRs) are important targets for treating severe diseases. However why certain molecules act as activators whereas others, with similar structures, block GPCR activation, is poorly understood since the same molecule can activate one receptor subtype while blocking another closely related receptor. To shed light on these central questions, we used all-atom, long-time-scale molecular dynamics simulations on the κ-opioid and μ-opioid receptors (κOR and μOR). We found that water molecules penetrating into the receptor interior mediate the activating versus blocking effects of a particular ligand–receptor interaction. Both the size and the flexibility of the bound ligand regulated water influx into the receptor. The solvent-accessible inner surface area was found to be a parameter that can help predict the function of the bound ligand.*

The known crystal structures of ligand-free and ligand-bound G-protein-coupled receptors (GPCRs), as well as their ternary complexes with G proteins, show a large number of structural details[1]. Based on static crystal structures and molecular dynamics simulations, some common elements in the activation mechanism of GPCRs have been found, including side-chain microswitches, movement of transmembrane helices, and rearrangement of internal water molecules.[2–7] Herein, we concentrate on the question of whether specific properties of GPCR ligands can be predicted from the structural features of the corresponding ligand–receptor complexes obtained from computer simulations.

Levallorphan is a morphine-like drug that is widely used as an antidote and opioid modulator.[8] It acts as an agonist for κ-opioid receptors (κORs) but as an antagonist for μ-opioid receptors (μORs).[9] As a result, it blocks the effects of stronger agents with greater intrinsic activity, such as morphine or endogenous β-endorphin.[10] To address the different effects of levallorphan on κORs and μORs, we first performed all-atom molecular dynamics (MD) simulations on the crystal structures of both the κOR (pdb: 4DJH)[11] and μOR (pdb: 4DKL)[12] (Table 1).

Table 1: Ligand–receptor systems used for MD simulations.

Receptor	κOR	κOR–jdt	κOR–lev	μOR–lev	μOR–mor
Ligand	–	JDTic	levallorphan	levallorphan	morphine
Function	apo	antagonist	agonist	antagonist	agonist
t [μs]	0.5	3	3	3	3

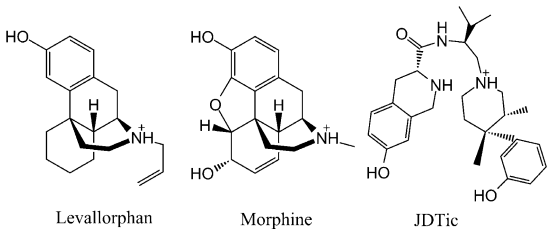

Our previous work[6] indicated that a Na^+ ion from bulk water can diffuse into the allosteric site of μOR, bind to the highly conserved $D114^{2.50}$, and thereby influence receptor function. To determine whether this finding would pertain to κOR, we performed 0.5 μs MD simulations for apo-κOR

[*] Dr. S. Yuan, Prof. H. Vogel
Ecole Polytechnique Fédérale de Lausanne (EPFL)
Institute of Chemical Sciences and Engineering
Lausanne (Switzerland)
E-mail: shuguang.yuan@gmail.com
horst.vogel@epfl.ch
Prof. K. Palczewski
Department of Pharmacology, School of Medicine
Case Western Reserve University, Cleveland (USA)
Dr. Q. Peng
Department of Chemistry, University of Oxford (UK)
Dr. M. Kolinski
Bioinformatics Laboratory, Mossakowski Medical Research Centre
Polish Academy of Sciences, Warsaw (Poland)
Prof. S. Filipek
Laboratory of Biomodeling, Faculty of Chemistry & Biological and Chemical Research Centre, University of Warsaw, Warsaw (Poland)
E-mail: sfilipek@chem.uw.edu.pl

[**] We thank the Pittsburgh Supercomputing Center in the USA for use of the Anton supercomputer system (NIH grant RC2GM093307) to support the major computing part of this project (grant PSCA12032P). Part of the work was done at the Shanghai Supercomputer Center and Interdisciplinary Centre for Mathematical and Computational Modelling in Warsaw as grant G07-13. S.F. received funding from National Center of Science, Poland, grant no. 2011/03/B/NZ1/03204. Research in H.V.'s group was supported by the Swiss National Science Foundation (grant 31003A-133141), the European Community (project SynSignal, grant no. FP7-KBBE-2013-613879), and internal funds of the EPFL. H.V. and S.F. participate in the European COST Action CM1207 (GLISTEN).

Supporting information for this article is available on the WWW under http://dx.doi.org/10.1002/anie.201501742

(Figure S1 in the Supporting Information). As expected, a Na^+ ion penetrated into the inner space of κOR through the same three stages (Figure S1A,B) observed with apo-μOR.[6] We even found that the final position of this Na^+ ion inside κOR was similar to that in both the MD simulation structure of μOR[6] and the crystal structure of $A_{2A}R$[13] (Figure S1C). Because Na^+ ions play a crucial role in GPCR activation,[4,6] we placed a Na^+ ion at the allosteric site in all subsequent MD simulations.

Next, we examined conformational fluctuations in the ligand–receptor complexes. For the complex between κOR and its antagonist JDTic (κOR–jdt), two particular hydrogen bonds between JDTic and D138$^{3.32}$ were monitored over time (Figure 1): N1H–OD1 and N2H–OD2. These interactions were stable during the whole 3 μs MD simulation. A similar stability was observed for the complex between μOR and the antagonist levallorphan (μOR–lev), although only one hydrogen bond linked the ligand to D147$^{3.32}$. By contrast, the interactions in the receptor–agonist complexes κOR–lev and μOR–mor were less stable and dissociated during the MD simulations (Figure 1). In the case of κOR–lev, the interaction between the ligand and the receptor was already completely disrupted at 1.3 μs. For morphine, it flipped between OD1 and OD2.

Penetration of water molecules into the receptor interior has been found to be a hallmark of GPCR activation.[4–6] Compatible with this theme, we observed a distinct difference in the number of water molecules inside the receptor after the binding of an agonist or an antagonist (Figure 2 and Figure S2). The final structures obtained from MD simulations showed fewer water molecules at the ligand-binding and allosteric sites of μOR–lev (Figure 2C and Figure S2), with levallorphan acting as an antagonist, than in κOR–lev (Figure 2B and Figure S2), with levallorphan acting as an agonist. A similar characteristic was found for the binding of agonist and antagonist to the same receptor: in the antagonist-bound complex κOR–jdt, far fewer intrinsic water molecules were detected ($\langle N\rangle = 3\pm1$) than in agonist-bound κOR–lev ($\langle N\rangle = 9\pm2$; Figure 2A,B and Figure S2), and similarly for the antagonist complex μOR–lev and the agonist complex μOR–mor (Figure 2C,D and Figure S2). Interestingly, in μOR–lev, the ligand levallorphan fits tightly into the receptor binding site. Besides the formation of a hydrogen bond with D147$^{3.32}$, the hydrophobic tail of levallorphan at the protonated nitrogen interacts with Y320$^{7.43}$ to form σ–π stacking that blocks water penetration. Although a similar interaction was observed for the bound antagonist in the κOR–jdt complex (Figure 2A), this was missing for the bound agonists in the κOR–lev and μOR–mor complexes. This implies that the size of the ligand in the binding pocket determines whether it acts as an agonist or an antagonist. Thus an agonist occupies a smaller portion of the receptor binding pocket than does an antagonist, and the binding flexibility of particular ligands induces an influx of solvent molecules into the inner space of the receptor as an initial step of activation.[4,6] By contrast, antagonists occupy a comparatively larger portion of the binding pocket space, thereby blocking the entrance of water molecules. The residue Y$^{7.43}$, which is

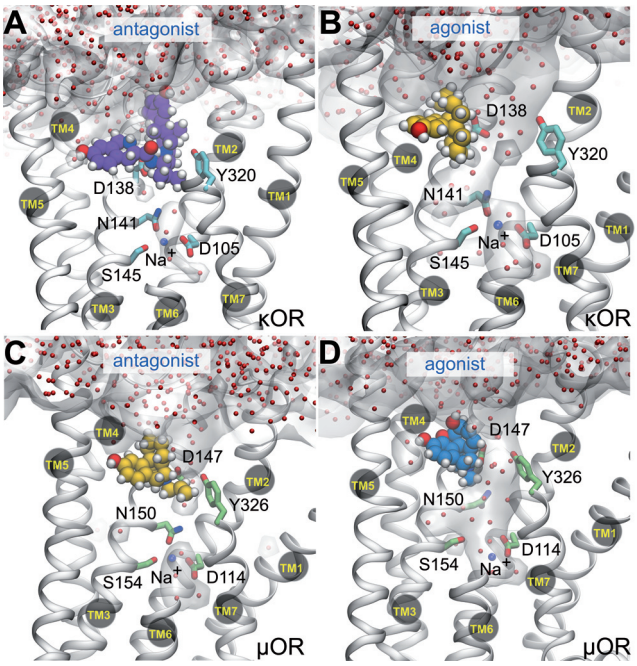

Figure 2. Water inside κOR (top) and μOR (bottom) at the end of the 3-μs MD simulations. Red dots = water molecules; blue dots = Na^+ ions. A) κOR with bound antagonist JDTic (purple carbon atoms). B) κOR with bound agonist levallorphan (orange carbon atoms). C) μOR with bound antagonist levallorphan (orange carbon atoms). D) μOR with bound agonist morphine (blue carbon atoms). For both receptors, the average number of water molecules in the ligand binding pocket was $\langle N\rangle = 3\pm1$ for the antagonist complexes and $\langle N\rangle = 9\pm2$ for the agonist complexes.

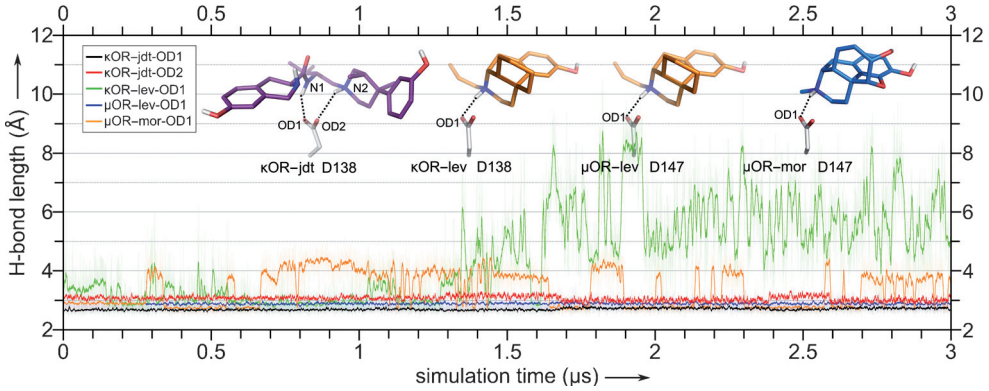

Figure 1. Lengths of the hydrogen bonds between the ligand and D$^{3.32}$ in the receptor binding pocket during 3-μs MD simulation. Purple stick model = JDTic; orange stick model = levallorphan; blue stick model = morphine. Plots of hydrogen-bond lengths are depicted in black (κOR-OD1–jdt; OD1 is one oxygen atom of the carboxylic group in the side chain of D138), red (κOR-OD2–jdt; OD2 is the second oxygen atom of the carboxylic group in the side chain of D138), green (κOR-OD1–lev), blue (μOR-OD1–lev), and orange (μOR-OD1–mor).

bound tightly by antagonists, also fluctuates in agonist-bound complexes. The hydrogen bond between $D^{3.32}$ and $Y^{7.43}$ breaks and re-forms, which facilitates the influx of water and rearrangement of the hydrogen bond network. The role of the $Y^{7.43}$ residue was found to be important for the activation of opioid receptors in our earlier studies,[14] even without its role in water influx. The transient movements of $Y^{7.43}$ are in line with movements of the $W^{6.48}$ residue, which opens a gate for water.[9] Here, $Y^{7.43}$ forms another gate, so the pipeline of water can participate in activation of the receptor.

To identify the relationship between ligand properties and the formation of a water pathway, we calculated the solvent accessible surface area (SASA) of the receptor in its extracellular binding pocket based on our final 5 ns MD simulations. We found that the SASA values for the antagonist-bound complexes κOR–jdt (350 Å^2) and μOR–lev (450 Å^2) were distinctly smaller for particular receptor types than those for the agonist-bound complexes κOR–lev (480 Å^2) and μOR–mor (590 Å^2), respectively. To confirm this conclusion, we performed 20 ns MD simulations for each of 69 compounds (Figure S3–6), including 16 κOR agonists, 19 κOR antagonists, 18 μOR agonists, and 16 μOR antagonists from a GPCR-ligand database.[15] The receptor starting structures for μOR and κOR were the same in all cases. The final 2 ns MD simulations showed that the SASA values for most of the κOR agonists were in the range of 450–700 Å^2 (Figure 3), whereas the SASA values for the κOR antagonists were in the range of 300–460 Å^2. Following the same pattern, the SASA values for agonist-bound μOR (Figure S7) were in the range of 600–750 Å^2, while those for antagonist-bound μOR were in the range of 400–650 Å^2. These differences are statistically significant with a two-tail p-value of 1.30×10^{-6} for κOR and 1.45×10^{-5} for μOR. We thus conclude that the SASA values of the receptor binding pocket are larger for complexes with agonists than with antagonists.

Helix bending is another hallmark of GPCR activation.[4,5,16] This was also evident in the final 60 ns period of each of our MD simulations: both agonist-bound complexes κOR–lev and μOR–mor underwent characteristic helix bending in TM6 (Figure S8) and TM7 (Figure S9), which was missing in the antagonist-bound complexes κOR–jdt and μOR–lev. The D/ERY ionic lock between TM3 and TM6 has been considered to play a crucial role in GPCR activation.[17,18] We also observed a D/ERY ionic lock switch (Figure S10). The ionic salt bridge between $D^{3.49}$ and $R^{3.50}$ in the agonist-bound complexes κOR–lev and μOR–mor was broken at approximately 1.0 μs and 0.6 μs, respectively. By contrast, this salt bridge was stable during the whole MD simulation for both antagonist-bound complexes κOR–jdt and μOR–lev.

In conclusion, our MD simulations revealed the structural basis of agonist/antagonist sensing for both κOR and μOR

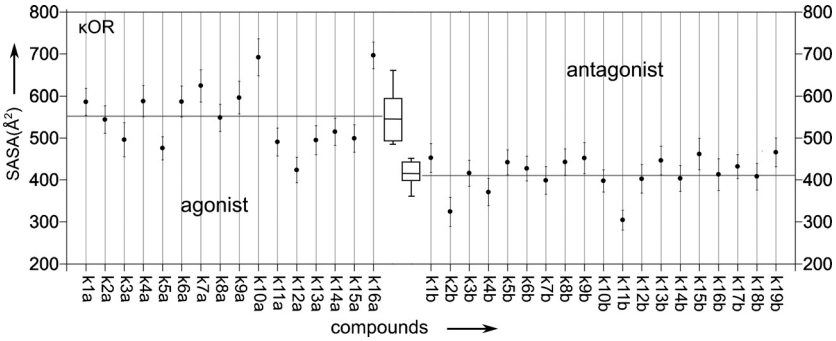

Figure 3. Solvent accessible surface areas (SASA) values for agonist-bound κOR (left panel) and antagonist-bound κOR (right panel). Error bars represent standard deviations obtained from statistical evaluation of 200 snapshots extracted from the final parts of the MD simulations. Values were calculated based on the final 2 ns of 35 20-ns MD simulations. SASA values for κOR with agonists are in the range of 450–700 Å^2, with a mean value of 560 ± 65 Å^2 (left horizontal line); whereas for κOR with antagonists, the values are in the range of 300–460 Å^2, with a mean value of 415 ± 43 Å^2 (right horizontal line). Distributions of data points for the two ligand sets are presented by box-and-whisker plots: a box represents the 25%–75% distribution range of the corresponding data points depicting the median inside; the whisker represents the 10%–90% distribution range. The chemical structures of the compounds are shown in Figures S3 and S4.

(Figure 4). Levallorphan behaved as an agonist for κOR by inducing unstable binding with $D^{3.32}$ and subsequent water penetration owing to the large SASA of the κOR–lev complex. By contrast, levallorphan was stabilized in the binding site of μOR by hydrogen bonding to $D^{3.32}$ and a σ–π interaction with $Y^{7.43}$. This combination blocked the entry of water molecules from the bulk environment because of the comparatively smaller SASA of the μOR–lev complex relative to κOR–lev. Owing to differences in the structures of the binding sites of receptors that differ more than closely related subtypes, a direct comparison of their SASA values may be risky. Considering the same receptor type, the binding of antagonists generally results in smaller SASA values for the

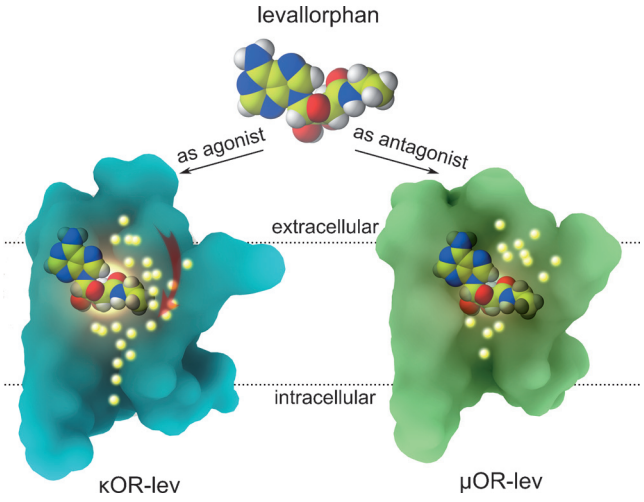

Figure 4. Schematic representation of ligand binding in κOR and μOR. Levallorphan (yellow-green carbon atoms) acts as an agonist in κOR owing to the large SASA of κOR–lev, which allows the penetration of water molecules (yellow dots) required for receptor activation. In contrast, levallorphan acts as an antagonist in μOR because the decreased SASA value of μOR-lev leads to blocking of water entry into the receptor.

receptors binding pocket than those for agonist-bound complexes. This characteristic property may be useful for computational screening of GPCR ligands, however, the involvement of MD simulations means that it is presently not a rapid screening method. The movement of water, along with a simultaneous rearrangement of the internal hydrogen-bond network, could be the major driving force of receptor activation. In this interpretation, the action of molecular switches would be derived from the ligand–receptor match and the ability of water to enter the receptor.

Experimental Section

Our membrane system was built by a membrane embedding tool in Maestro,[19] with each receptor crystal structure pre-aligned in the OPM (Orientations of Proteins in Membranes) database.[20,21] Pre-equilibrated 154 POPC lipids coupled with 12000 TIP3P water molecules in a periodic box of $80 \times 80 \times 104$ Å were used to build the protein/membrane system. Proteins, lipids, water molecules, and ions were modeled with the CHARMM36 force field[22] parameter set; the ligands were modeled with the CHARMM CGenFF small-molecule force field.[23] All ligands were submitted to the GAUSSIAN09 program[24] for structure optimization at the B3LYP/6-31G* level prior to force field parameter generation. All bond lengths to hydrogen atoms in each protein/membrane system were constrained with M-SHAKE.[25] Van der Waals and short-range electrostatic interactions were cut off at 10 Å. The long-time-scale MD simulations were performed in Desmond[26] at the specialized supercomputer ANTON.[27] Results obtained from the MD simulations were analyzed in Gromacs[28] and VMD.[29] The bending of helices was calculated in Bendix[30] with default settings.

Keywords: GPCRs · molecular dynamics · protein models · receptors · signal transduction

How to cite: *Angew. Chem. Int. Ed.* **2015**, *54*, 7560–7563
Angew. Chem. **2015**, *127*, 7670–7673

[1] A. J. Venkatakrishnan, X. Deupi, G. Lebon, C. G. Tate, G. F. Schertler, M. M. Babu, *Nature* **2013**, *494*, 185.
[2] V. Katritch, V. Cherezov, R. C. Stevens, *Annu. Rev. Pharmacol. Toxicol.* **2013**, *53*, 531.
[3] R. O. Dror, R. M. Dirks, J. P. Grossman, H. Xu, D. E. Shaw, *Annu. Rev. Biophys.* **2012**, *41*, 429.
[4] S. Yuan, S. Filipek, K. Palczewski, H. Vogel, *Nat. Commun.* **2014**, *5*, 4733.
[5] S. Yuan, Z. Hu, S. Filipek, H. Vogel, *Angew. Chem. Int. Ed.* **2015**, *54*, 556–559; *Angew. Chem.* **2015**, *127*, 566–569.
[6] S. Yuan, H. Vogel, S. Filipek, *Angew. Chem. Int. Ed.* **2013**, *52*, 10112; *Angew. Chem.* **2013**, *125*, 10299.
[7] A. S. Rose, M. Elgeti, U. Zachariae, H. Grubmuller, K. P. Hofmann, P. Scheerer, P. W. Hildebrand, *J. Am. Chem. Soc.* **2014**, *136*, 11244.
[8] B. Raton, *Index Nominum 2000: International Drug Directory*, Medpharm Scientific Publishers, **2000**.
[9] L. L. Brunton, J. S. Lazo, K. Parker in *The Pharmacological Basis of Therapeutics*, 12th ed. (Eds.: L. L. Brunton, J. S. Lazo, K. Parker), McGraw-Hill Professional, **2011**, p. 602.
[10] E. E. Codd, R. P. Shank, J. J. Schupsky, R. B. Raffa, *J. Pharmacol. Exp. Ther.* **1995**, *274*, 1263.
[11] H. Wu, D. Wacker, M. Mileni, V. Katritch, G. W. Han, E. Vardy, W. Liu, A. A. Thompson, X. P. Huang, F. I. Carroll, S. W. Mascarella, R. B. Westkaemper, P. D. Mosier, B. L. Roth, V. Cherezov, R. C. Stevens, *Nature* **2012**, *485*, 327.
[12] A. Manglik, A. C. Kruse, T. S. Kobilka, F. S. Thian, J. M. Mathiesen, R. K. Sunahara, L. Pardo, W. I. Weis, B. K. Kobilka, S. Granier, *Nature* **2012**, *485*, 321.
[13] W. Liu, E. Chun, A. A. Thompson, P. Chubukov, F. Xu, V. Katritch, G. W. Han, C. B. Roth, L. H. Heitman, A. P. IJzerman, V. Cherezov, R. C. Stevens, *Science* **2012**, *337*, 232.
[14] M. Kolinski, S. Filipek, *J. Mol. Model.* **2010**, *16*, 1567.
[15] Y. Okuno, A. Tamon, H. Yabuuchi, S. Niijima, Y. Minowa, K. Tonomura, R. Kunimoto, C. Feng, *Nucleic Acids Res.* **2008**, *36*, D907.
[16] B. Trzaskowski, D. Latek, S. Yuan, U. Ghoshdastider, A. Debinski, S. Filipek, *Curr. Med. Chem.* **2012**, *19*, 1090.
[17] K. Palczewski, T. Orban, *Annu. Rev. Neurosci.* **2013**, *36*, 139.
[18] X. Deupi, B. K. Kobilka, *Physiology* **2010**, *25*, 293.
[19] Maestro, version 9.6, Schrödinger, LLC, New York, NY, **2013**.
[20] A. L. Lomize, I. D. Pogozheva, H. I. Mosberg, *J. Chem. Inf. Model.* **2011**, *51*, 918.
[21] A. L. Lomize, I. D. Pogozheva, H. I. Mosberg, *J. Chem. Inf. Model.* **2011**, *51*, 930.
[22] J. B. Klauda, R. M. Venable, J. A. Freites, J. W. O'Connor, D. J. Tobias, C. Mondragon-Ramirez, I. Vorobyov, A. D. MacKerell, R. W. Pastor, *J. Phys. Chem. B* **2010**, *114*, 7830.
[23] K. Vanommeslaeghe, E. P. Raman, A. D. MacKerell, Jr., *J. Chem. Inf. Model.* **2012**, *52*, 3155.
[24] M. J. Frisch, G. W. Trucks, H. B. Schlegel, G. E. Scuseria, M. A. Robb, J. R. Cheeseman, G. Scalmani, V. Barone, B. Mennucci, G. A. Petersson, H. Nakatsuji, M. Caricato, X. Li, H. P. Hratchian, A. F. Izmaylov, J. Bloino, G. Zheng, J. L. Sonnenberg, M. Hada, M. Ehara, K. Toyota, R. Fukuda, J. Hasegawa, M. Ishida, T. Nakajima, Y. Honda, O. Kitao, H. Nakai, T. Vreven, J. A. Montgomery, Jr., J. E. Peralta, F. Ogliaro, M. J. Bearpark, J. Heyd, E. N. Brothers, K. N. Kudin, V. N. Staroverov, R. Kobayashi, J. Normand, K. Raghavachari, A. P. Rendell, J. C. Burant, S. S. Iyengar, J. Tomasi, M. Cossi, N. Rega, N. J. Millam, M. Klene, J. E. Knox, J. B. Cross, V. Bakken, C. Adamo, J. Jaramillo, R. Gomperts, R. E. Stratmann, O. Yazyev, A. J. Austin, R. Cammi, C. Pomelli, J. W. Ochterski, R. L. Martin, K. Morokuma, V. G. Zakrzewski, G. A. Voth, P. Salvador, J. J. Dannenberg, S. Dapprich, A. D. Daniels, Ö. Farkas, J. B. Foresman, J. V. Ortiz, J. Cioslowski, D. J. Fox, Gaussian, version 2009, Gaussian, Inc., Wallingford, CT, USA, **2009**.
[25] E. Barth, K. Kuczera, B. Leimkuhler, R. D. Skeel, *J. Comput. Chem.* **1995**, *16*, 1192.
[26] C. A. R. Edmond Chow, K. J. Bowers, R. O. Dror, D. H. Hughes, J. Gullingsrud, F. D. Sacerdoti, and D. E. Shaw, DESRES/TR-2008-01 ed., D. E. Shaw Research, D. E. Shaw Research Technical Report, **2008**.
[27] D. E. Shaw, R. O. Dror, J. K. Salmon, J. P. Grossman, K. M. Mackenzie, J. A. Bank, C. Young, M. M. Deneroff, B. Batson, K. J. Bowers, E. Chow, M. P. Eastwood, D. J. Ierardi, J. L. Klepeis, J. S. Kuskin, R. H. Larson, K. Lindorff-Larsen, P. Maragakis, M. A. Moraes, S. Piana, Y. Shan, B. Towles in *ACM/IEEE Conference on Supercomputing (SC09)*, New York, **2009**.
[28] S. Pronk, S. Pall, R. Schulz, P. Larsson, P. Bjelkmar, R. Apostolov, M. R. Shirts, J. C. Smith, P. M. Kasson, D. van der Spoel, B. Hess, E. Lindahl, *Bioinformatics* **2013**, *29*, 845.
[29] W. Humphrey, A. Dalke, K. Schulten, *J. Mol. Grap. & Mod.* **1996**, *14*, 33; Mod. **1996**, 14, 33.
[30] A. C. E. Dahl, M. Chavent, M. S. P. Sansom, *Bioinformatics* **2012**, *28*, 2193.

Received: February 23, 2015
Revised: March 30, 2015
Published online: May 12, 2015

